

Catalytic performance and mechanism of meso-microporous material Beta-SBA-15 supported FeZr catalysts for CO₂ desorption in CO₂ loaded aqueous amine solution

Yufei Huang[†], Xiaowen Zhang, Hongxia Gao*, Yangqiang Huang, Paitoon Tontiwachwuthikul, Zhiwu Liang*

Joint International Center for CO₂ Capture and Storage (iCCS), Provincial Hunan Key Laboratory for Cost-effective Utilization of Fossil Fuel Aimed at Reducing CO₂ Emissions, College of Chemistry and Chemical Engineering, Hunan University, Changsha 410082, PR China * Author for correspondence:

Email: hxgao@hnu.edu.cn, zwliang@hnu.edu.cn (Dr. Z Liang)

ABSTRACT

The highly energy requirement of rich amine solvent regeneration process is the biggest obstacle for the industrial application of amine-based CO₂ capture technology. In this work, to reduce the heat duty of absorbent regeneration, the zeolite Beta/SBA-15 (BS) with different zeolite Beta (β) content synthesized by the hydrothermal method with zeolite Beta (β) as the silicon source were utilized to prepare the novel Zr@BS and Fe-Zr@BS catalysts for amine regeneration. Experiments for CO₂ stripping were performed under the temperature of 370.15 K using amine solvent (monoethanolamine (MEA)) with an initial CO₂ loading of 0.5 mol CO₂/mol amine. Additionally, various techniques including X-ray diffraction (XRD), Fourier transform infrared spectroscopy (FT-IR), N₂ adsorption-desorption experiment, ammonia temperature programmed desorption (NH₃-TPD), and pyridine-adsorption infrared spectroscopy (Py-IR) were adopted to characterize and estimate the prepared catalysts. Also, the catalytic CO₂ desorption performances of seven different catalysts (β , SBA-15, three BS catalysts, Zr@BS and Fe-Zr@BS) were investigated and evaluated in terms of the cyclic capacity, desorption rate and energy consumption. The experimental results showed that the Fe-Zr@BS catalysts exhibited best catalytic performance than other catalysts studied in this work, enhancing the desorption factor by 212% and reducing the energy consumption by 33% compared to the blank run. Furthermore, the Fe-Zr@BS catalysts have no influence on the amine absorption performance in terms of the absorption rate and have the advantages of good stability and easy regeneration. Based on the results of characterization and experiments, the possible catalytic mechanism for the

Fe-Zr@BS catalysts catalyzed amine regeneration for CO₂ stripping were proposed and the reusability of the catalysts were also investigated.

Keywords: CO₂ capture, catalysts, MEA, desorption, heat duty, acid sites.

NONMENCLATURE

<i>Abbreviations</i>	
β	zeolite Beta
BS	zeolite Beta/SBA-15
MEA	monoethanolamine
XRD	X-ray diffraction
FT-IR	Fourier transform infrared spectroscopy
NH ₃ -TPD	Ammonia temperature programmed desorption
Py-IR	Pyridine-adsorption infrared spectroscopy
CCUS	carbon capture utilization and storage
TEOS	Tetraethyl orthosilicate
P123	EO ₂₀ PO ₇₀ EO ₂₀
Q_c , in mol	Cyclic capacity
α	mol CO ₂ /mol amine
HD, kJ/mol	Heat duty
DF, mol ³ /(kJ·min)	Desorption factor
MSA, m ² /g	Mesopore surface area
BAS, mmol/g	Brønsted acid sites
LAS, mmol/g	Lewis acid sites

Selection and peer-review under responsibility of the scientific committee of the 11th Int. Conf. on Applied Energy (ICAE2019).

Copyright © 2019 ICAE

1. INTRODUCTION

It was generally accepted that a large amount of CO₂ from the combustion of fossil fuels releasing into atmosphere has resulted in many environmental issues, and has been considered as one of major contributions to global warming[1, 2]. Hence, it has become imperative to control CO₂ emission in the atmosphere. Among several existing technologies for carbon capture utilization and storage (CCUS), amine-based chemical absorption is the most selective and advanced technique, having attracted the most attention, due to its high absorption kinetics, relative low solvent cost and unique flexibility[3, 4]. However, its virtues tend to be stifled by the solvent degradation, equipment corrosion and the large heat requirement in the overall CO₂ desorption processes, resulting the most critical challenge for implementation of carbon capture utilization and storage technology[5-8]. Therefore, current researches are focused on reducing the heat duty of MEA solvent regeneration for CO₂ capture to ensure that the technology is accepted globally without significant economic losses[9, 10].

Recently, extensive efforts have done to create metallic oxide catalysts to reduce the energy requirement for amine regeneration process. Bhatti et al.[11-13] have reported the application of various transition metal oxide catalysts to MEA solvent regeneration for CO₂ stripping, reducing the sensible heat by 25%-48% in MEA solvent regeneration process comparing to the blank run. However, Lai et al[14]. have pointed out that MoO₃ and V₂O₅ react and dissolve in the rich amine solution, and the TiO₂ studied in that work had only marginal effects. Zhang et al.[15] and Liu et al.[16] presented finding that SO₄²⁻/TiO₂ and SO₄²⁻/ZrO₂ can reduce the heat duty of amine regeneration by 17% and 10% compared to that without catalyst, respectively. Nevertheless, it's relatively small surface area and irregular pore structure resulting a critical challenge for the real application of amine solvent regeneration for CO₂ stripping.

In addition, some studies have been reported that use of molecular sieve catalysts (HZSM, HY, SAPO-34, MCM-41) in MEA regeneration is the effective approach to minimize the heat requirement for MEA solvent regeneration[10, 15, 17]. The results showed that HZSM can reduce the heat duty of amine regeneration by 40% due to its acid sites altering the reaction path of MEA solvent regeneration for CO₂ stripping. Yet, its limitation is associated with the fewer acid sites, which has necessitated the development of many other

catalysts with high catalytic activity. Zhang et al.[18, 19] reported that SO₄²⁻/ZrO₂/γ-Al₂O₃ and Al₂O₃/HZSM-5 can also reduce the energy consumption of MEA regeneration by 25%-37% respectively, comparing to the baseline solvent MEA. The studies reveal that the composite catalysts can greatly improve amine desorption performance due to high acid sites, large surface area and large pores. However, some major drawbacks, namely, the reusability of the composite catalysts, has posed barriers for the real application of amine solvent regeneration for CO₂ stripping.

In overcome the limitation of metallic oxide catalysts and individual molecular sieve materials in the CO₂ desorption for amine regeneration process, it's very important to design the novel hierarchically porous composite materials combing the advantageous of molecular sieve and metallic oxide. It is well known that SBA-15 has large pores, large surface area and good thermal stability compared with other mesoporous materials, factors which facilitate the introduction of metals into the framework[20, 21]. However, the pure SBA-15 molecular sieve has little acid sites, and this is detrimental to the amine regeneration process. In order to overcome this problem, the introduction of β molecular sieve into SBA-15 support might enhance the catalytic performance of SBA-15 by increasing the number of catalytically acid sites and improving the rate of mass-transfer.

In this research, the novel composite materials zeolite Beta /SBA-15 (BS) with different zeolite Beta (β) content, Zr@BS and Fe-Zr@BS catalysts were synthesized by the hydrothermal method for amine regeneration. Seven different catalysts were compared for their amine desorption performance in terms of reaction rate, heat duty, cyclic capacity and CO₂ absorption rate. Additionally, the structure, surface area, and characteristics of the catalysts were elucidated by various characterization approaches, i.e. XRD, FT-IR, N₂ adsorption-desorption, NH₃-TPD, and Py-IR. Based on the characterization data of the catalysts and the CO₂ desorption experiments, possible catalytic mechanisms for Fe-Zr@BS catalyzed amine regeneration for CO₂ stripping were proposed. Furthermore, the reusability of the bifunctional catalysts was also investigated.

2. EXPERIMENTAL SECTION

2.1 Chemicals

MEA (purity of 99%) and NH₃·H₂O (purity of 28-30%) were obtained from Shanghai Aladdin Industrial Corporation, China. Tetraethyl orthosilicate (TEOS, 98%)

and EO₂₀PO₇₀EO₂₀ (Pluronic P123) were got from Shanghai Aladdin Biochemical Technology Co. Ltd., China. β molecular sieves were purchased from Tianjin NanKai University Catalyst Co. Ltd., China. Zirconium oxychloride hydrate (ZrOCl₂·8H₂O, purity of 98%) were provided by Shanghai Macklin Biochemical Co. Ltd., China. Hydrochloric acid (HCl, 36-38%) and Ferric nitrate nonahydrate (Fe(NO₃)₃·9H₂O, 98.5%) were acquired from Sinopharm Chemical Reagent Co. Ltd, China. CO₂ (purity of 99.9%) and N₂ (purity of 99.99%) were obtained from Changsha Jingxiang Gas Co. Ltd., China. Methyl orange (0.10%wt) indicator was acquired from Tianjin Kermel Chemical Reagent Co. Ltd., China. All materials were used without further purification.

2.2 Preparation of catalysts

The meso-microporous material BS were obtained using TEOS as the silica source and EO₂₀PO₇₀EO₂₀ (P123) as the template by the hydrothermal method from the reported in the literature with some modified[22, 23]. Typically, 9.81g of P123 was added into deionized water and stirred at 315 K for 1 h, and then 588.73 g of 6M hydrochloric was introduced into mixture solution and stirred for 2 h at 315 K. Finally, an amount 6 g of β molecular sieves was added and the mixture was stirred for 2 h at 315 K, and 20.80 g of TEOS was put into the solution at 315K and stirred for 24 h. Afterward, the mixture was transferred into a stainless autoclave and crystallized at 383.15 K for 48 h. After the hydrothermal reaction, the products were filtered and washed with distilled water, then dried at 373.15 K under air for 12 h and calcined at 823 K under air with a ramping rate of 5 K/min for 6 h.

The novel composite materials Zr@BS and Fe-Zr@BS were synthesized by precipitation method. Firstly, 10.0 g of BS material was introduced into the 100 g of water and stirred at room temperature, and then the certain amount Fe(NO₃)₃·9H₂O and ZrOCl₂·8H₂O were added into the mixture, under ultrasonic conditions for 0.5 h. Moreover, the NH₃·H₂O was introduced into solution until the system pH arrived 8-9 under vigorously stirring at room temperature for 3 h. Afterward, the resulting precipitates were filtered and washed with distilled water, followed by drying, and sintering at 823 K for 6 h.

For the comparison, the pure SBA-15 molecular sieves were synthesized, in which the procedure was similar to that of the BS method, without addition of β into solution.

2.3 Experimental apparatus and procedure

2.3.1 CO₂ Desorption Experiment

A schematic diagram of experimental apparatus for the amine regeneration is illustrated in Figure 1. It can be obtained that the experiment apparatus consisted of a 1L round-bottom flask equipped with one thermometer, a condenser, a mass flow meters, an oil bath, a power meter, an infrared CO₂ analyzer and a tube for inlet gases. The oil bath (model DF-101S, Yuhua, China, with $\pm 1.0\%$ F.S. accuracy) was used to provide the desired energy for the amine regeneration and CO₂ stripping. A condenser at the top of the flask was applied to condense the mixture gas and keep the concentration of amine solution. A mass flow meter (model D07, Beijing Sevenstar, China) was used for controlling the flow rate of N₂, which was mixed with the CO₂ desorbed from rich amine solution. An infrared CO₂ analyzer with $\pm 1.0\%$ F.S. accuracy (model GS10, Ennix, Germany) was applied to determine the concentration of CO₂ in mixed gas. In addition, the energy consumption of amine solvent regeneration for CO₂ desorption was measured by the power meter (Zhejiang Tepsung electric Co. Ltd., China, accuracy of 0.001 kW/h, and uncertainty of ± 0.1 kW/h).

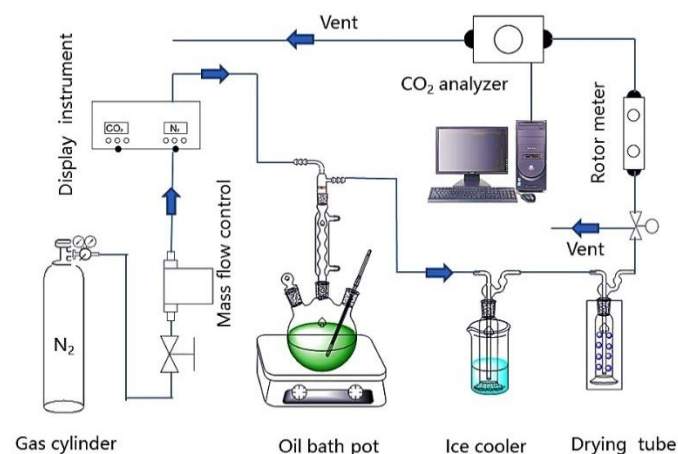


Figure 1. Schematic diagram of experimental device for amine solution regeneration process.

For each amine solution regeneration experiment, 6.25 ± 0.01 g catalyst and 500 mL of 5M MEA solution with the rich loading of 0.50 mol CO₂/mol amine were introduced into the 1000 mL of batch reactor. Secondly, the first data of CO₂ concentration desorbed from rich amine solution was recorded when the temperature of amine solution arrived at 328 K with stirring rate of 1200 rpm, keeping the sufficient interfacial contact area of gas and liquid, and maintaining the desired desorption temperature of amine solution. Moreover, it can be obtained that it took 1 h to raise the temperature of

amine solution from 328.15 K to 370.15 K, and then the temperature of solution was kept constantly at 370.15 K. The mixed gas, i.e. CO₂ desorbed from rich amine and N₂ drawn from the compressed gas cylinders at flow rate of 450 mL/min, was introduced into the infrared CO₂ analyzer to determine the concentration of CO₂ at an interval of one minute. The energy consumption of amine regeneration for CO₂ desorption were determined by the power meter at the experimental run time of 1h.

2.3.2 CO₂ Absorption Experiment

A schematic diagram of amine solution absorption experiment, with the purpose of evaluating the catalytic performance of amine absorption for catalysts. This experiments apparatus had been described in detail in our previous investigation by Gao et al[24]. For each absorption experiment, the water bath was heated at 313.15 K and the stirring speed was set at 1200 rpm. Then, 300 mL of CO₂-unloaded amine solution with 3.75 of catalysts placed into the flask was applied to absorb the CO₂ from the mixed gas, constituting of the CO₂ and N₂ with the flow rates 150 and 850 mL/min respectively. Afterward, the mixed gas was dried by silica and then introduced into the infrared CO₂ analyzer to measure the concentration of CO₂ at an interval of one minute. Moreover, in order to ensure the reliability of data in this absorption experiment, the CO₂ loading of the liquid samples was also determined by titration using 1 mol/L HCl at least two times.

2.4 Theory

The instantaneous CO₂ desorption rate (r , mol/(s*L)) was determined by the flow rates of outlet and inlet gases, as presented in Equations 1.

$$r = \frac{1}{V} (n_{CO_2}^{in} - \frac{X_{CO_2}^{out}}{1-X_{CO_2}^{out}} \cdot n_{N_2}) \quad (1)$$

Here, V is the volume of amine regeneration solution, $n_{CO_2}^{in}$ and n_{N_2} is molar rate of CO₂ and N₂ of the feed gas, respectively, and the $X_{CO_2}^{out}$ represents the mole fraction of CO₂ in the outlet gas.

The amount of CO₂ desorbed from rich amine with the gas method and liquid defined as the cyclic capacity (Q_C , in mol), as illustrated in Equation 3.

$$\alpha_{lean} = \alpha_{rich} - \frac{r \cdot \Delta X_{CO_2} \cdot 60}{C} \quad (2)$$

$$Q_C = (\alpha_{rich} - \alpha_{lean}) * C * V \quad (3)$$

where α_{lean} and α_{rich} is the CO₂ loading of the initial amine solution and the amine solution after regeneration, respectively; ΔX_{CO_2} represents the mole

fraction changes of CO₂ in the outlet gas, monitoring by the CO₂ analyzer; and C is the concentration of amine regeneration solution.

The CO₂ desorption rate (\bar{r} , mol/min) can be defined as the amount of CO₂ stripped from the solvent over a specific period time, as shown in Equation 4.

$$\bar{r} = \frac{Q_C}{t} \quad (4)$$

where t is 60 minutes in this work.

The heat duty (HD , kJ/mol) is the amount of energy consumption for each mole of CO₂ desorbed from loaded amine solution, as displayed in Equation 5. The relative heat duty (RH , %), representing that the mole fraction of energy consumption for amine regeneration with different catalysts compared with that of blank experiment, was calculated in Equation 6.

$$HD = \frac{E/t}{Q_C/t} \quad (5)$$

$$RH = \frac{HD}{HD_{baseline}} \times 100 \quad (6)$$

where E is the amount of energy consumed for amine regeneration with different catalysts over a specific period time, and $HD_{baseline}$ represents the amount of energy consumed for amine regeneration with catalyst-free over a specific period time.

In addition, a desorption factor (DF , mol³/(kJ·min)) is a comprehensive parameter to evaluate the performance of catalysts during CO₂ desorption, as presented in Equation 7.

$$DF = \frac{\bar{r} \cdot Q_C}{HD} \quad (7)$$

2.5 Catalyst Characterization

X-ray diffraction (XRD) patterns of the supports and the composite catalysts were performed on XRD-600 and Rigaku Ultimate IV using Cu Ka radiation as an X-ray source, and then the data were collected in the ranges of 0.5°-10° and 10°-80° corresponding to the scan rate of 0.5°/min rate of 1 min⁻¹ in steps of 8°.

FT-IR spectra of catalysts were obtained by a Vector 22 Fourier Transform infrared using KBr wafer technique in the wavelength range of 400-3000cm⁻¹ to investigate the functional groups in the materials in this work.

The N₂ adsorption desorption isotherms were recorded at 77K on Micromeritics ASAP 2460 instrument to study the physical property of catalyst including surface area, total pore volume and average pore diameter. The materials were first degassed at 473.15 K for 5h. The specific surface areas were determined by the BET method, and the average pore diameters and the

cumulative volumes of pores were obtained using Barrett-Joyner-Halenda (BJH) method.

FTIR spectra of adsorbed pyridine of sample (Py-IR) was performed on Thermoscientific-Nicolet-IS-10 to evaluate the nature and acid amount of catalysts. Prior to each test, the catalyst was heated for 120 minutes in vacuum at 523.15 K followed by cooled to room temperature for a pyridine adsorption experiment.

Temperature-programmed desorption of carbon dioxide (NH₃-TPD) measurements were carried out by Micromeritics 2920II to evaluate the overall density of the acid sites for sample.

3. RESULTS AND DISCUSSION

3.1 Catalyst Characterization

3.1.1 Structural and Physical Properties

Figure 2a and Figure 2b showed the XRD patterns of the supports and the composite catalysts. It was obviously found that the three characteristic diffraction peaks in the small-angle region were emerged in SBA-15 catalysts, corresponding to d_{100} , d_{110} and d_{200} planes, demonstrating the characteristics of P6mm hexagonal mesoporous material of SBA-15 materials[25, 26]. There were only one peak corresponding to d_{110} planes appearing in the composite catalysts, attributing to the carbon skeleton to shrink of composite catalysts with the introduction of β molecular sieve into SBA-15[27]. It was also obtained from Figure 2b that both supports and the composites catalysts show an intense peak at $2\theta = 22.50^\circ$ and 43.88° , indicating the composites catalysts own the structures of SBA-15 and β molecular sieve. However, the Zr@BS and Fe-Zr@BS catalysts displayed no diffraction lines for zirconia and iron oxide respectively, indicating the active metals were highly dispersed on the support surface as well as loaded into the pores of the molecular sieve[28].

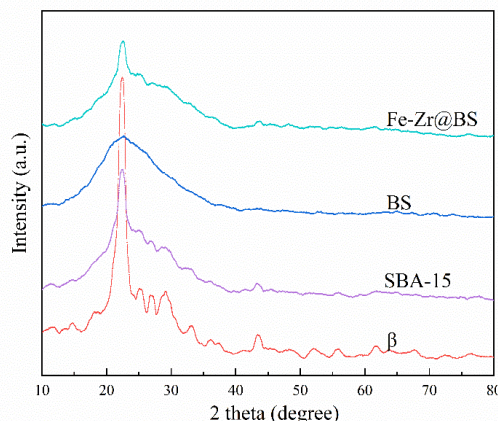
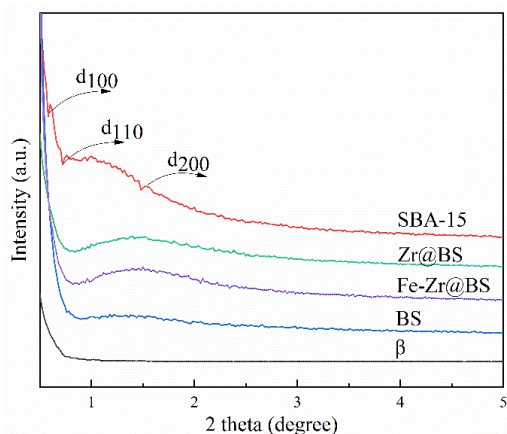


Figure 2. XRD patterns of various catalysts (Planes a and b are small angle and wide angle XRD patterns of supports and composite catalysts, respectively).

The FT-IR spectra of the supports and the composite catalysts are presented in Figure 3. It can be learned that the shoulder of SBA-15 centered at 460 cm^{-1} , 800 cm^{-1} and 1100 cm^{-1} , attributing to the bending modes of Si-O-Si, symmetric stretching and asymmetric stretching respectively, and then, the band at 965 cm^{-1} is due to stretch vibration of non-bridged Si-OH[29, 30]. In β molecular sieve, the bands at 523 cm^{-1} and 574 cm^{-1} were attributed to the vibration of the double four-membered ring of β molecular sieve[31], and the shoulder at 623 cm^{-1} is attributed to the vibration of the five-membered ring[32]. It was remarkable that five shoulders centered at 523 cm^{-1} , 574 cm^{-1} , 800 cm^{-1} , 965 cm^{-1} and 1100 cm^{-1} were observed in the FT-IR spectra of composite materials BS, indicating the secondary structural unit of the β molecular sieve introduction the skeleton structure of the composite molecular sieve. Moreover, it can be observed that the shoulders at 600 cm^{-1} and 965 cm^{-1} were gradually illegible with incorporation of zirconium and iron oxide into the structure of mesoporous material, demonstrating the association of Si-OH and active metals to Si-O-Zr groups and Si-O-Fe groups[28].

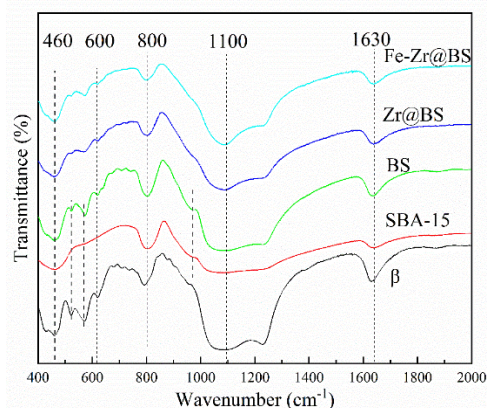


Figure 3. Infrared spectra of supports and metal-containing BS samples.

The N₂ adsorption-desorption isotherms of supports and the composite catalysts were investigated and presented in Figure 4, corresponding to specific surface area, Pore volume and the pore diameter of samples showed in Table 1. It can be obtained that the isotherms of all samples were of Type IV with a marked leap based on the IUPAC classification, which is one of the main characteristics of mesoporous materials[33]. The micropore surface areas and mesopore surface areas of BS catalysts increased from 30.83 m²/g to 260.59 m²/g and from 158.27 m²/g to 461.12 m²/g comparing to the SBA-15 and β molecular sieve respectively, demonstrating the BS catalysts have microporous and mesoporous channels. In addition, it can be also learned from Figure 4 and Table 1 that the surface areas and pore volumes of composite catalysts (Zr@BS, Fe-Zr@BS) decreased with introduction of active metals into BS materials, indicating the zirconium and iron oxide were coated on the pore surface or the pore channel of composite molecular sieve.

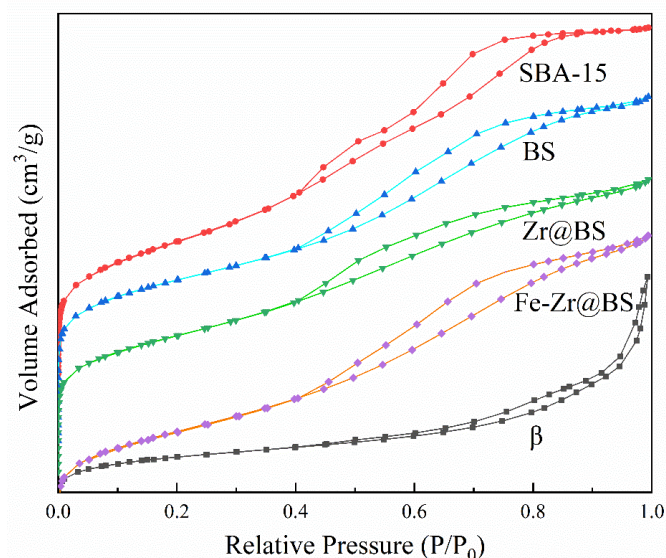


Figure 4. N₂ adsorption-desorption isotherms of supports and composite catalysts.

Table 1. The textural characteristics of the catalysts.

Sample	S _{Micro} ^a (m ² /g)	S _{Meso} ^b (m ² /g)	S _{BET} ^c (m ² /g)	PV (cm ³ /g)	AD (nm)
β	469.17	158.27	654.94	0.66	4.04
SBA-15	30.83	586.78	617.61	0.68	4.40
BS	260.59	461.12	721.72	0.68	3.77
Zr@BS	164.63	462.18	626.81	0.58	3.70
Fe-Zr@BS	147.47	461.23	608.70	0.64	3.50

S_{Micro}^a is the micropore surface area.

S_{Meso}^b represents mesoporous surface area.

$$S_{BET}^c = S_{Micro}^a + S_{Meso}^b.$$

3.1.2 Acidity and Basicity of Catalysts

The FT-IR spectra after pyridine adsorption on supports and composite catalysts were investigated to distinguish Bronsted and Lewis acid sites, as presented in Figure 5. The characteristic bands at 1540 cm⁻¹ and 1450 cm⁻¹ were observed, which can be assigned to the pyridine adsorption on Bronsted acid sites and Lewis acid sites, respectively[21, 34]. The concentration of Bronsted acid sites and Lewis acid sites were calculated from the integral intensities of the typical bands and the acidity of catalysts were displayed in Table 2. It was interestingly noted that the concentration of Bronsted acid sites and Lewis acid sites of BS increased by 525.71% and 477.22% comparing with that SBA-15 molecular sieve, respectively. Moreover, the composite catalysts pose more Bronsted acid sites than BS, increasing by 179.35% and 261.14%. Judging from the intensities of the bands observed in the FT-IR spectra, the orders of the Bronsted acid sites and total acidities of catalysts studied in this work are follows as: β > Fe-Zr@BS > Zr@BS > BS > SBA-15 > Blank, and β > BS > Zr@BS > Fe-Zr@BS > SBA-15 > Blank.

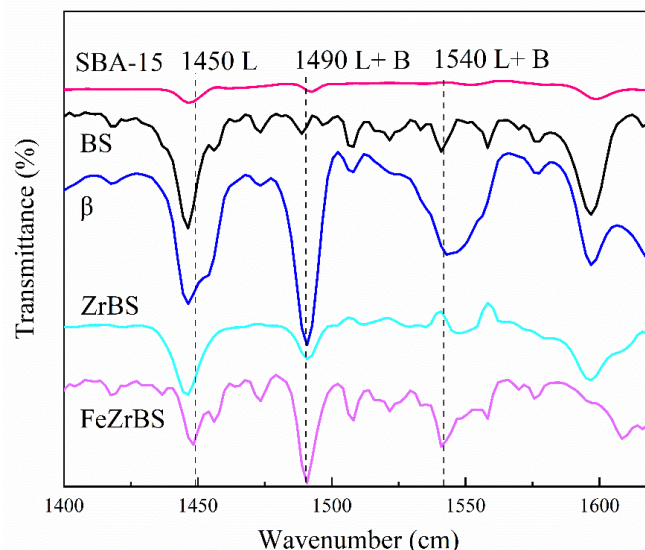


Figure 5. FTIR-pyridine spectra of catalysts.

Table 2. acid properties of different catalysts (mmol/g).

catalysts	BAS	LAS	B/L	Total
	(mmol/g)	(mmol/g)		(mmol/g)
β	15.94	12.36	1.29	28.30
SBA-15	0.35	2.89	0.12	3.24
BS	1.84	10.41	0.18	12.25
Zr@BS	3.30	7.44	0.44	10.75
Fe-Zr@BS	4.81	3.56	1.35	8.37

NH₃-TPD experiments were carried out to obtain the acidity of the catalysts, and the results were reported in Figure 6 and Table 3. The amount of NH₃ desorbed from materials at a temperature range can be regarded as a measure of concentration of acid sites and the acid strength distribution on the samples. It was noted that all the samples showed a peak at 413.15 K, indicating the weak surface acidic sites of catalysts[30]. For supports, there were no obvious characteristic peaks when the temperature raised from 413.15 to 903.15K. Nevertheless, the BS catalysts show two peaks at 573.15 K and 903.15 K, supporting the medium strong acid sites and strong acid sites on the BS materials[35]. Moreover, the composite catalysts display a second desorption peak at temperature of 903.15 K, attributing to the interaction of NH₃ with strong acid sites.

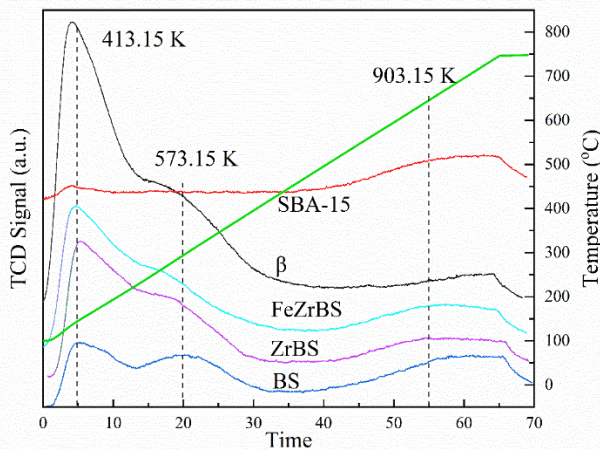


Figure 6. NH₃-TPD curves of molecular sieve, Zr@BS and Fe-Zr@BS.

Table 3. NH₃-TPD amounts of acidic sites (mmol/g).

catalyst	Weak (mmol/g)	Strong (mmol/g)	Super strong (mmol/g)	total (mmol/g)
β	0.72	0	0.15	0.87
SBA-15	0.02	0	0.12	0.14
BS	0.17	0.20	0.24	0.61
Zr@BS	0.24	0	0.26	0.50
Fe-Zr@BS	0.34	0	0.27	0.61

3.2 CO₂ Desorption Performance

It is well known that the desorption rate and energy requirement are important parameters for evaluating the catalytic performance of catalysts in the MEA solution regeneration process. The relative energy requirement for 5 M MEA solution regeneration without catalysts was regarded as 100% as the baseline. The SBA-15 modified by β with different mass ratio of β and SBA-15 was employed to evaluate its catalytic performance on MEA regeneration in terms of the desorption rate and

energy consumption, as presented in Figures 7a and 7b. From Figure 7, it was observed that both SBA-15 and β can facilitate the CO₂ release and reduce the energy consumption of amine regeneration compared with the baseline solvent MEA (without catalysts). Moreover, it also showed that the novel composite materials BS display better catalytic performance than that of the individual molecular sieve, which can minimize the heat duty for MEA solvent regeneration by 12%-20% compared with the blank run. As revealed in Figure 7a and 7b, it can be learned that the CO₂ desorption rate and relative heat duty of amine regeneration are ranked in the order as: BS(50%) > BS(20%) > BS(80%) > SBA-15 > β > Blank, and BS(50%) < BS(20%) < SBA-15 < BS(80%) < β < Blank. The experimental results revealed that the BS(50%) catalyst exhibited the better catalytic activity among all tested BS catalysts, resulting in a reduction of 20% in terms of energy consumption of amine solution regeneration compared with the blank run.

Hence, in order to further enhance the catalytic performance of BS (50%) material for CO₂ desorption of MEA solvent, the BS(50%) modified by the ZrO₂ and Fe₃O₄ were prepared and employed in the MEA regeneration process to evaluate its catalytic activity, as shown in Figure 7c and 7d. Based on Figure 7c and 7d, it was clear that the introduction of ZrO₂ into BS can further improve the CO₂ desorption rate and lower the heat duty of MEA regeneration process. In addition, it was noted that the Fe-Zr@BS catalyst presented superior catalytic performance among the investigated catalysts in this work, reducing the heat duty of MEA solvent regeneration by 33% comparing with the blank run. The orders of the CO₂ desorption rate and energy consumption for amine regeneration for the tested catalysts are follows as: Fe-Zr@BS > Zr@BS > BS > Blank, and Fe-Zr@BS < Zr@BS < BS < Blank.

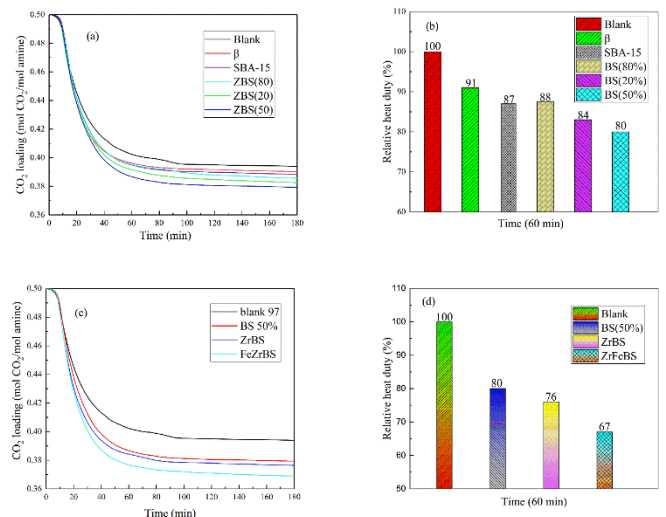


Figure 7. Catalytic CO₂ desorption performance in MEA solution at 370.15K (Panels a and c are the graphs for catalytic performance of catalysts; Graph b and d are the relative heat duty).

Moreover, it is notable that the *DF* is a comprehensive parameter to evaluate the performance of catalysts during CO₂ desorption using 5 M MEA solution. The *DF* of MEA solvent with different catalysts are shown in Figure 8, it was clearly that the *DF* of MEA solvent improved by 16.67%-48.68% with the addition of BS catalysts into MEA system, and then, further enhanced by 64.03% and 122.81% with the introduction of Zr@BS catalysts and Fe-Zr@BS catalysts into the MEA regeneration process, respectively. From Figure 8, the *DF* with different catalysts shows the order of: Fe-Zr@BS > Zr@BS > BS(50%) > BS(20%) > SBA-15 > BS(80%) > β > Blank.

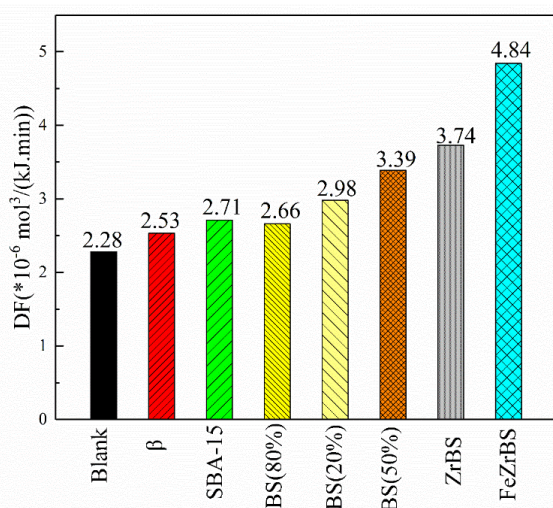


Figure 8. The *DF* of MEA solution regeneration at 370.15 K with or without catalysts.

Based on the experiment results, the relationship of the physicochemical properties of the catalysts between with the performance of amine regeneration for CO₂ stripping were investigated. The experimental results indicated that the catalytic performance of SBA -15 is better than that of β, possessing the most the mesopore surface areas in all catalysts studied in this work. It can be concluded that the mesopore surface areas of catalysts plays important role in the amine regeneration. On the other hand, the concentration of BAS and the super strong acid sites play a leading role in the catalytic effect of catalyst for amine regeneration process, as increasing of mesoporous specific. It can be learned from Figure 9a and 9b that the energy consumption of the amine solution decreases and the desorption rate increases with the increase in number of the BAS and super strong acid sites. In summary, the catalytic performance of catalyst for amine regeneration

increased with the increasing of the BAS, super strong acid sites and the mesopore surface areas.

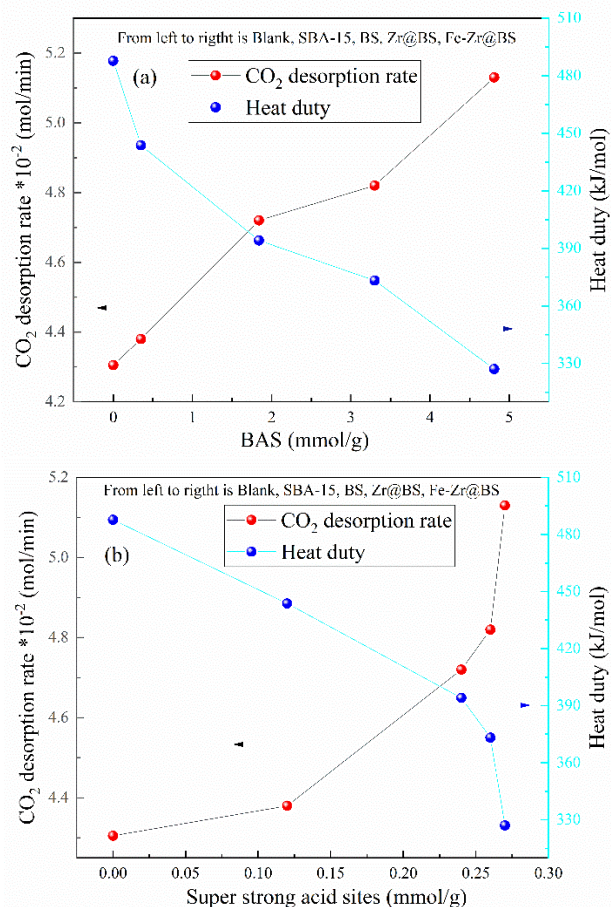


Figure 9. The influence of catalysts properties on performance of amine regeneration (graphs a and BAS and super strong acid sites, respectively).

3.3 CO₂ Absorption Performance

The influence of the novel composite materials Fe-Zr@BS on the CO₂ absorption behavior of 5 M MEA solution was also investigated, and then, the typical CO₂ absorption profile of MEA solvent with or without catalysts at the absorption temperature of 313K is displayed in Figure 10. Based on the Figure 10, it can be clearly that the CO₂ loading greatly increase with the absorption time and equilibrium at 0.50 mol CO₂/mol amine about 200 minutes. The experiment results revived that the two curves display the same change trends in terms of CO₂ absorption rate, demonstrating catalysts studied in this work have no negative influence on the CO₂ absorption behavior of 5 M MEA solution.

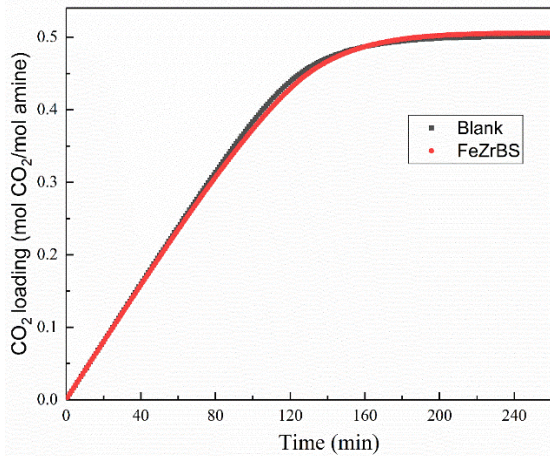


Figure 10. Influence of catalyst on absorption performance of MEA solution.

3.4 Reliability of Experimental Setup and Catalysts

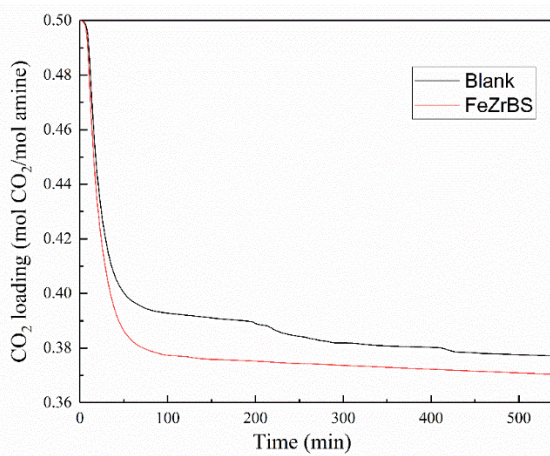


Figure 11. Experimental regeneration curves in the liquid phase for loading change.

The reliability of desorption apparatus was evaluated by the gas-liquid material balance. The average absolute relative deviation (AARD) of the CO₂ loadings of aqueous MEA solution taken at 0, 0.5, 1 and 2 h calculated by the concentration of CO₂ in the gas phase and the titration is 1.0970%, indicating the accuracy and reliability of the experimental set-up.

The typical CO₂ desorption profile of 5 M MEA solution with or without catalysts in the temperature range of the 328.15K-370.15K is presented in Figure 11. It can be obtained that the slope of CO₂ desorption profile decreased sharply in the initial 60 minutes, and then the slope turned less sharply in the next 120 minutes, and then tended to be constant after 540 minutes of experiments. It can be also learned that the addition of Fe-Zr@BS catalysts into amine regeneration process can significantly improve CO₂ desorption kinetics in the initial 200 minutes, and then the CO₂ desorption rate has little change and tend to be constant in the next 340 minutes.

It also revived a fact that the synthesized catalysts in this work just facilitated the desorption kinetics and not as a reaction in the present work.

3.5 Catalyst Stability

The stability of Fe-Zr@BS catalyst was evaluated with five cycle CO₂ desorption experiment in terms of desorption rate and energy consumption, as presented in Figure 12. The spent catalysts used in amine regeneration process were first washed by distilled water and followed by dried in the drying at 373.15 K in for 12 h before addition into the 5 M solution for CO₂ stripping. As shown in Figure 12, it can be observed that the catalytic performance of Fe-Zr@BS catalyst after five times amine regeneration process display little change in terms of desorption rate and energy consumption, confirming that Fe-Zr@BS catalyst shows a good stability.

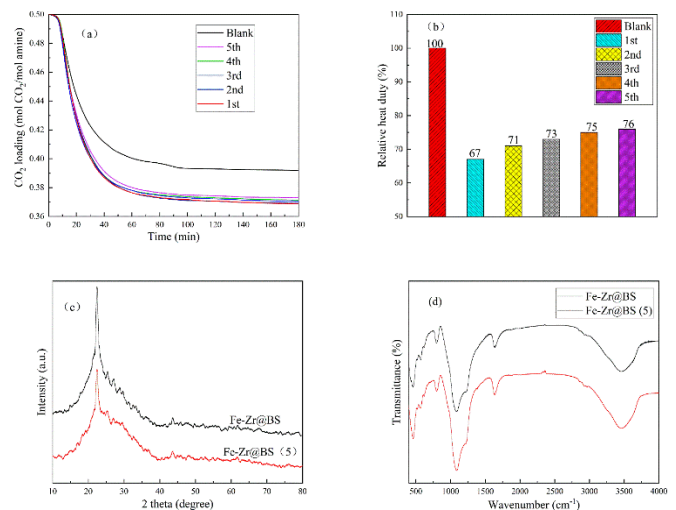


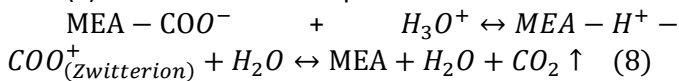
Figure 12. Catalyzed cyclic CO₂ desorption (graphs of a and b are CO₂ desorption rate and relative heat duty; poles c and d are XRD patten and FT-IR spectra of Fe-Zr@BS).

In addition, the physicochemical properties of Fe-Zr@BS catalysts after recycling five times were also studied by the XRD and FT-IR methods, as presented in Figure 12c and 12d. It can be obtained from Figure 12c that the diffraction peaks of the Fe-Zr@BS (5) catalyst have no changes compared with blank catalysts, demonstrating the microporous and mesoporous channels of Fe-Zr@BS still retained. Moreover, it can be also learned from the Figure 12d that the FT-IR peaks of Fe-Zr@BS catalysts were unchanged after recycling many times, which supported that the functional group of Fe-Zr@BS almost unchanged. In summary, it can be concluded that the Fe-Zr@BS catalysts synthesized in this work has good stability, considering the catalytic performance and the structure.

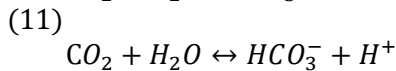
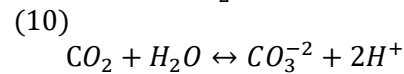
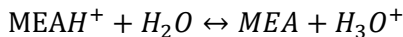
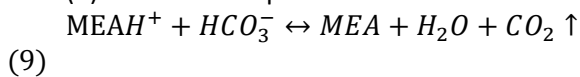
3.6 Catalytic Mechanism

The process of CO₂ absorption and CO₂ desorption in MEA solution can be explained well by the zwitterion mechanism[36, 37]. The zwitterion theory, consisted of (a) carbamate breakdown (MEACOO⁻) and (b) the process of protonated amine (MEA⁺H) deprotonation, was supported from the analytical means of NMR spectrum. The possible reactions in MEA regeneration process without catalysts were presented in Equations 8-12. Based on the zwitterion theory, it can be obtained that the great deal energy was required in amine regeneration process, attributing to the difficulty of transferring the proton from protonated and strongly endothermic reaction (Equation 8). Moreover, the HCO₃⁻ group as a catalyst can involve in the proton donating or accepting reaction to alter the reaction path of the deprotonation of AmineH⁺, resulting the faster desorption rate and lesser energy consumption[16].

(a) Carbamate breaks up to form zwitterions



(b) AmineH⁺ deprotonation



Based on the research discussed above, the possible catalytic mechanism for composite catalysts in rich amine regeneration process was proposed, as illustrated in Figure 13. On the one hand, the HCO₃⁻ group as a catalyst can transfer the proton from AmineH⁺ to water to produce MEA and the available proton. On the other hand, the composite catalysts process can accelerate the MEACOO⁻ breakdown to reduce the energy required for amine regeneration.

First, the MEACOO⁻, passed through the channel of the composite catalysts and obtained the proton from the BAS and LAS of catalysts, were converted into MEA-COOH (1). Then, O atom bonds to metal atoms after the chemisorption takes places on the MEA-COOH and composite catalysts, attributing to the mass transfer on external and internal of MEA-COOH and catalysts (2). Afterword, the hydrogen atom (H) on the oxygen (O) dislocates the O, and then H shifts to the neighbouring of N atom to convert into zwitterion - metal atoms with the effects of isomerization (3). Fourth, the protons (BAS) and the metal atom (LAS) on the catalysts can rob the lone pair electron of N atom and destroy the de-localized

conjugation[12], breaking the conjugation of the carbamate not only by switching from SP² to SP³ formation, but also, by lengthening the N-C bond to weaken the bond strength (4). Finally, the zwitterion splits into the MEA and CO₂ as the effect of C-N bond breakdown (5).

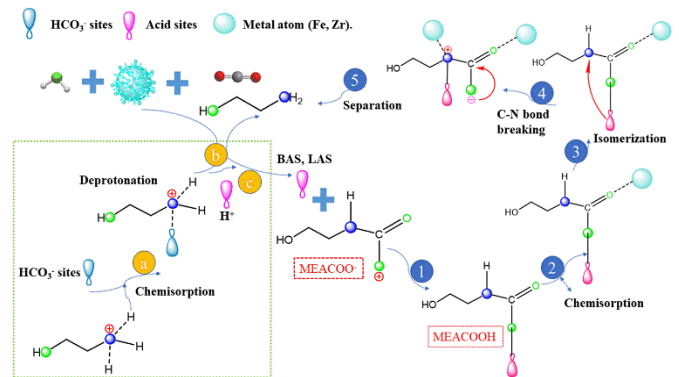


Figure 13. The possible catalytic mechanism for Fe-Zr@BS in rich amine regeneration process.

4. CONCLUSIONS

In this work, the solvent regeneration performance of Seven different catalysts was investigated in terms of heat duty and CO₂ desorption rate. The catalytic activities of these catalysts decreased in the order as: Fe-Zr@BS > Zr@BS > BS (50%) > BS (20%) > BS (80%) > SBA-15 > β > blank run. The experimental results showed that Fe-Zr@BS can enhance the desorption factor by 212% and reduce the energy consumption by 33% compared with the blank experiment. In addition, a possible catalytic amine solvent regeneration mechanism was suggested over the catalyst Fe-Zr@BS. Furthermore, Fe-Zr@BS catalyst has good stability and has no adverse influence on the CO₂ absorption performance of amine solution. Findings from this work demonstrated that Fe-Zr@BS has the advantages of higher catalytic performance, easy separation and good stability, indications that it has great potential for application in industrial CO₂ capture process.

ACKNOWLEDGEMENT

The financial support from the National Natural Science Foundation of China (NSFC-Nos. 21536003, 21706057, 21606078 and 51521006), the Natural Science Foundation of Hunan Province in China (No. 2018JJ3033), and the China Outstanding Engineer Training Plan for Students of Chemical Engineering & Technology in Hunan University (MOE-No. 2011-40).

REFERENCE

- [1] Wu H, Gao L, Jin H, Li S. Low-energy-penalty principles of CO₂ capture in polygeneration systems. *Applied Energy*. 2017;203:571-81.
- [2] Xie W, Chen X, Ma J, Liu D, Cai T, Wu Y. Energy analyses and process integration of coal-fired power plant with CO₂ capture using sodium-based dry sorbents. *Applied Energy*. 2019;252:113434.
- [3] Ji L, Yu H, Li K, Yu B, Grigore M, Yang Q, et al. Integrated absorption-mineralisation for low-energy CO₂ capture and sequestration. *Applied energy*. 2018;225:356-66.
- [4] Li K, Jiang K, Jones TW, Feron PH, Bennett RD, Hollenkamp AF. CO₂ regenerative battery for energy harvesting from ammonia-based post-combustion CO₂ capture. *Applied energy*. 2019;247:417-25.
- [5] Zhang S, Shen Y, Shao P, Chen J, Wang L. Kinetics, thermodynamics, and mechanism of a novel biphasic solvent for CO₂ capture from flue gas. *Environmental science & technology*. 2018;52:3660-8.
- [6] Zhang S, Du M, Shao P, Wang L, Ye J, Chen J, et al. Carbonic anhydrase enzyme-MOFs composite with a superior catalytic performance to promote CO₂ absorption into tertiary amine solution. *Environmental science & technology*. 2018;52:12708-16.
- [7] Barzagli F, Lai S, Mani F, Stoppioni P. Novel non-aqueous amine solvents for biogas upgrading. *Energy & Fuels*. 2014;28:5252-8.
- [8] Ling H, Gao H, Liang Z. Comprehensive solubility of N₂O and mass transfer studies on an effective reactive N, N-dimethylethanolamine (DMEA) solvent for post-combustion CO₂ capture. *Chemical Engineering Journal*. 2019;355:369-79.
- [9] Li K, van der Poel P, Conway W, Jiang K, Puxty G, Yu H, et al. Mechanism investigation of advanced metal-ion-mediated amine regeneration: a novel pathway to reducing CO₂ reaction enthalpy in amine-based CO₂ capture. *Environmental science & technology*. 2018;52:14538-46.
- [10] Liang Z, Idem R, Tontiwachwuthikul P, Yu F, Liu H, Rongwong W. Experimental study on the solvent regeneration of a CO₂-loaded MEA solution using single and hybrid solid acid catalysts. *AIChE Journal*. 2016;62:753-65.
- [11] Bhatti UH, Shah AK, Kim JN, You JK, Choi SH, Lim DH, et al. Effects of transition metal oxide catalysts on MEA solvent regeneration for the post-combustion carbon capture process. *ACS Sustainable Chemistry & Engineering*. 2017;5:5862-8.
- [12] Bhatti UH, Nam S, Park S, Baek IH. Performance and mechanism of metal oxide catalyst-aided amine solvent regeneration. *ACS Sustainable Chemistry & Engineering*. 2018;6:12079-87.
- [13] Bhatti UH, Sivanesan D, Lim DH, Nam SC, Park S, Baek IH. Metal oxide catalyst-aided solvent regeneration: A promising method to economize post-combustion CO₂ capture process. *Journal of the Taiwan Institute of Chemical Engineers*. 2018;93:150-7.
- [14] Lai Q, Toan S, Assiri MA, Cheng H, Russell AG, Adidharma H, et al. Catalyst-TiO (OH)₂ could drastically reduce the energy consumption of CO₂ capture. *Nature communications*. 2018;9:2672.
- [15] Zhang X, Zhang X, Liu H, Li W, Xiao M, Gao H, et al. Reduction of energy requirement of CO₂ desorption from a rich CO₂-loaded MEA solution by using solid acid catalysts. *Applied Energy*. 2017;202:673-84.
- [16] Liu H, Zhang X, Gao H, Liang Z, Idem R, Tontiwachwuthikul P. Investigation of CO₂ regeneration in single and blended amine solvents with and without catalyst. *Industrial & Engineering Chemistry Research*. 2017;56:7656-64.
- [17] Idem R, Shi H, Gelowitz D, Tontiwachwuthikul P. Catalytic method and apparatus for separating a gaseous component from an incoming gas stream. *Google Patents*; 2017.
- [18] Zhang X, Hong J, Liu H, Luo X, Olson W, Tontiwachwuthikul P, et al. SO₄²⁻/ZrO₂ supported on γ-Al₂O₃ as a catalyst for CO₂ desorption from CO₂-loaded monoethanolamine solutions. *AIChE Journal*. 2018;64:3988-4001.
- [19] Zhang X, Liu H, Liang Z, Idem R, Tontiwachwuthikul P, Al-Marri MJ, et al. Reducing energy consumption of CO₂ desorption in CO₂-loaded aqueous amine solution using Al₂O₃/HZSM-5 bifunctional catalysts. *Applied energy*. 2018;229:562-76.
- [20] Barbera K, Lanzafame P, Pistone A, Millesi S, Malandrino G, Gulino A, et al. The role of oxide location in HMF etherification with ethanol over sulfated ZrO₂ supported on SBA-15. *Journal of catalysis*. 2015;323:19-32.
- [21] Zhang Y, Chen Y, Pan J, Liu M, Jin P, Yan Y. Synthesis and evaluation of acid-base bi-functionalized SBA-15 catalyst for biomass energy conversion. *Chemical Engineering Journal*. 2017;313:1593-606.
- [22] Liu J, Liu J, Zhao Z, Tan J, Wei Y, Song W. Fe/Beta@SBA-15 core-shell catalyst: Interface stable effect and propene poisoning resistance for no abatement. *AIChE Journal*. 2018;64:3967-78.
- [23] Zhang D, Duan A, Zhao Z, Wang X, Jiang G, Liu J, et al. Synthesis, characterization and catalytic performance of meso-microporous material Beta-SBA-15-supported

NiMo catalysts for hydrodesulfurization of dibenzothiophene. *Catalysis today*. 2011;175:477-84.

[24] Gao H, Wu Z, Liu H, Luo X, Liang Z. Experimental studies on the effect of tertiary amine promoters in aqueous monoethanolamine (MEA) solutions on the absorption/stripping performances in post-combustion CO₂ capture. *Energy & fuels*. 2017;31:13883-91.

[25] Zhao D, Feng J, Huo Q, Melosh N, Fredrickson GH, Chmelka BF, et al. Triblock copolymer syntheses of mesoporous silica with periodic 50 to 300 angstrom pores. *science*. 1998;279:548-52.

[26] Zhao D, Huo Q, Feng J, Chmelka BF, Stucky GD. Nonionic triblock and star diblock copolymer and oligomeric surfactant syntheses of highly ordered, hydrothermally stable, mesoporous silica structures. *Journal of the American Chemical Society*. 1998;120:6024-36.

[27] Garg S, Soni K, Kumaran GM, Bal R, Gora-Marek K, Gupta J, et al. Acidity and catalytic activities of sulfated zirconia inside SBA-15. *Catalysis Today*. 2009;141:125-9.

[28] Chang B, Fu J, Tian Y, Dong X. Mesoporous solid acid catalysts of sulfated zirconia/SBA-15 derived from a vapor-induced hydrolysis route. *Applied Catalysis A: General*. 2012;437:149-54.

[29] Xie W, Zhao L. Heterogeneous CaO–MoO₃–SBA-15 catalysts for biodiesel production from soybean oil. *Energy conversion and management*. 2014;79:34-42.

[30] Chen W-H, Ko H-H, Sakthivel A, Huang S-J, Liu S-H, Lo A-Y, et al. A solid-state NMR, FT-IR and TPD study on acid properties of sulfated and metal-promoted zirconia: Influence of promoter and sulfation treatment. *Catalysis Today*. 2006;116:111-20.

[31] Zhang D, Duan A, Zhao Z, Xu C. Synthesis, characterization, and catalytic performance of NiMo catalysts supported on hierarchically porous Beta-KIT-6 material in the hydrodesulfurization of dibenzothiophene. *Journal of Catalysis*. 2010;274:273-86.

[32] Joaquin P, Johan A, Peter A. Crystallization mechanism of zeolite beta from (TEA)₂O, Na₂O and K₂O containing aluminosilicate gels. *Applied Catalysis*. 1987;31:35-64.

[33] Walton KS, Snurr RQ. Applicability of the BET method for determining surface areas of microporous metal-organic frameworks. *Journal of the American Chemical Society*. 2007;129:8552-6.

[34] Zhu S, Qiu Y, Zhu Y, Hao S, Zheng H, Li Y. Hydrogenolysis of glycerol to 1, 3-propanediol over bifunctional catalysts containing Pt and heteropolyacids. *Catalysis today*. 2013;212:120-6.

[35] Zhao J, Yue Y, Hua W, He H, Gao Z. Catalytic activities and properties of sulfated zirconia supported on mesostructured γ -Al₂O₃. *Applied Catalysis A: General*. 2008;336:133-9.

[36] Lv B, Guo B, Zhou Z, Jing G. Mechanisms of CO₂ capture into monoethanolamine solution with different CO₂ loading during the absorption/desorption processes. *Environmental science & technology*. 2015;49:10728-35.

[37] Caplow M. Kinetics of carbamate formation and breakdown. *Journal of the American Chemical Society*. 1968;90:6795-803.